13th Australasian Fluid Mechanics Conference
Monash University, Melbourne, Australia
13-18 December 1998

ENTRAINMENT PHENOMENA ASSOCIATED WITH MULTI-LIQUID FLOW OVER A WEIR

Peter LIOVIC[1], Murray RUDMAN[2], George ASSAAD[1], and Jong-Leng LIOW[1]

[1] GK Williams Cooperative Research Centre for Extractive Metallurgy
Department of Chemical Engineering
The University of Melbourne, Parkville, Victoria, AUSTRALIA

[2] CSIRO Division of Building, Construction and Engineering
Highett, Victoria, AUSTRALIA

ABSTRACT

The transient flow of immiscible liquid layers over a weir was investigated. The solution was calculated by solving the transient 2-D Cartesian equations of motion and continuity for incompressible flow, using the Volume of Fluid (VOF) method of Youngs (1982) and a stair-step representation of flow obstacles. Flow over a weir was investigated for the case where initially the liquid height of liquid is 25 percent greater than the weir height, while the liquid-liquid interface is located at a position 90 percent of weir height. Simulation results showed good agreement with experimental video images and measurements. Entrainment of the bottom liquid in the top liquid stream flowing over the weir occurred, despite the liquid-liquid interface initially being below the top of the weir.

INTRODUCTION

In a number of pyrometallurgical unit operations, there is a need to separate immiscible liquid layers. An important example is the need to separate waste slag from matte in the Peirce-Smith converter used in copper production. The converter is rotated and the overlying slag layer is poured out, leaving behind the valuable matte. It is desirable to remove only the slag during pouring, but matte entrainment makes this impossible. An understanding of entrainment during pouring processes would assist in optimising the loss of valuable matte to slag.

As a first step in studying the Peirce-Smith converter, we consider the flow of liquid over a weir. The study of the flow of immiscible liquid layers over a weir will provide an insight into entrainment seen in pouring operations in metallurgical processes. Although there is a large amount of literature of steady flows over a weir with one liquid, it was decided to test the code with a multi-liquid flow, as experimental data was readily available.

The presence of multiple fluids, complex fluid topologies and flow obstacles makes multi-liquid flow over a weir a challenging computational problem. Previous attempts at modelling this flow have been based on correlations and simplified flow models. No known attempts have been made to capture the heavy liquid entrainment associated with multi-liquid flow over a weir. Entrainment is a highly transient phenomenon, and steady state or averaged analogies to its modelling are totally inadequate. This means CFD simulation based on the full transient incompressible non-linear Navier-Stokes equations is required. Volume of Fluid (VOF) methods (Hirt and Nichols, 1981; Rudman, 1997) have proven to be valuable in simulating many real free surface flows, such as splash formation (Morton, 1997; Morton *et al.*, 1997) and jet-induced tank flows (Kothe *et al.*, 1991). The need to efficiently handle complex flow topologies and surface tension make VOF methods the best option for simulating flow over a weir.

NUMERICAL METHOD

Governing Equations

The numerical scheme directly solves the equations describing mass and momentum conservation for incompressible isothermal multi-fluid flows

$$\nabla.\mathbf{U} = 0 \tag{1}$$

$$\frac{\partial \mathbf{U}}{\partial t} + \nabla.\mathbf{UU} = -\frac{1}{\rho}\nabla \mathrm{P} + \frac{1}{\rho}\nabla.\tau + \mathbf{g} + S \tag{2}$$

where $\mathbf{U}$ is the velocity field, P is the pressure, τ is the viscous stress tensor, $\mathbf{g}$ is the gravity vector, S is the surface acceleration due to surface tension, and ρ is the density.

For flows involving multiple immiscible fluids, a colour function distribution is defined

$$C = \begin{cases} 1 & \text{in cells full of a particular fluid} \\ 0 & \text{in cells devoid of that particular fluid} \end{cases} \tag{3}$$

C takes the values $0 \le C \le 1$ on interfaces. For incompressible flow, species mass conservation requires C to satisfy

$$\frac{\partial C}{\partial t} + \nabla.(\mathbf{U}C) = 0 \tag{4}$$

Physical properties such as density and viscosity are recovered as weighted averages based on local values of C (for n fluid species and n-1 colour functions) -

$$\rho = \sum_{l=1}^{n-1} C_l \rho_l + \left(1 - \sum_{l=1}^{n-1} C_l\right)\rho_n \tag{5}$$

Solution Algorithm

A two-step projection is used to solve the governing equations. Given the values of all variables at time n, the solution is advanced to time n+1 as follows:

1. Determine the fluid topology by advecting all colour functions:

$$C^{n+1} = C^n - \delta t \nabla.\left(\mathbf{U}^n C^n\right) \qquad (6)$$

2. Compute new density and viscosity distributions using equations (5) and (6), based on C^{n+1}.

3. Make an initial estimate of the velocity field (**U***), based on the solution at time n (**U*** is typically not solenoidal)

$$\mathbf{U}^* = \mathbf{U}^n + \delta t \begin{bmatrix} -\nabla.(\mathbf{UU})^n - \frac{1}{\rho^n}\nabla P^n \\ +\frac{1}{\rho^n}\nabla.\tau^n + g + \frac{1}{\rho^n}\mathbf{S}^n \end{bmatrix} \qquad (7)$$

4. Solve the Poisson equation for the pressure correction (δP) to ensure continuity is satisfied

$$\nabla.\left(\frac{1}{\rho^n}\nabla\delta P\right) = \frac{1}{\delta t}\nabla.\mathbf{U}^* \qquad (8)$$

5. Update the velocity field and pressure distribution to time n+1

$$\mathbf{U}^{n+1} = \mathbf{U}^* - \frac{\delta t}{\rho^n}\nabla\delta P \qquad (9)$$

$$P^{n+1} = P^n + \delta P \qquad (10)$$

The solution algorithm as described in first order in time. Euler's improved time-stepping scheme is implemented to improve temporal accuracy to second order. Steps (3) to (5) are done twice - firstly with a half time-step, and secondly with a full time-step, but using values of **U**, P, ρ and μ from the half time-step solution.

The solution algorithm uses spatial discretisations based on a uniform staggered MAC mesh (Welch *et al.*, 1966). Scalar values are located at mesh cell centres, while velocities are located at the centre of cell edges. Discretisations of the equations in the solution algorithm are done using finite differences.

VOF Advection

The accuracy of VOF and interface tracking depend on the colour function advection scheme used. Best results are obtained using advection schemes specifically designed for colour function advection (Morton, 1997), rather than using arbitrary scalar advection schemes. The VOF advection scheme of Youngs (1982) has been shown to be accurate for VOF advection in two-dimensional flow simulations. This scheme is based on a piecewise linear reconstruction of interface cells, with interfacial line segment orientation estimated using weighted averaging based on *C* in surrounding cells. The method as first outlined by Youngs was only one-dimensional: direction splitting is implemented here to apply the procedure to two-dimensional flows.

Momentum Advection

In the momentum equations, centred differencing is used where possible in order to achieve second-order spatial accuracy. For the non-linear momentum advection terms however, centred differencing is unconditionally unstable. First-order upwinding, while stable, is unacceptably diffusive. In the code, a second-order van Leer's scheme is used (van Leer, 1977). Geometric limiters based on local gradients are computed to maintain stability by preserving monotonicity. The limiter is then used in combining second-order spatial accuracy from centred differencing with sufficient first-order upwinding to avoid instability.

Flow Obstacles

Obstacles to flow within the computational flow domain are modelled using a "stair-step" approach. Mesh cells lie either completely within the fluid or completely within the obstacle. Each fluid cell in the flow domain is flagged 1, while each obstacle cell is flagged 0. Using these flags enables fluid and obstacles cells to be distinguished. Boundary conditions are applied in obstacles cells flagged to be adjacent to fluid cells. Discretisations of the governing equations are modified to account for the control volume areas and cell faces blanked out by obstacles.

Pressure Correction Solver

Poisson's equation is discretised about mesh cell centres using a 5-point stencil. Neumann boundary conditions are set explicitly. The discretisation of Equation (8) yields a linear equation system of the form

$$Ax = b \qquad (11)$$

where the stiffness matrix *A* is a sparse, banded, symmetric and positive-definite matrix. Conjugate gradient (CG) methods are thus well suited to solving the linear equation system. A multigrid preconditioned conjugate gradient (MGCG) method was implemented, using the algorithm as outlined by Tatebe (1993). The preconditioning of the residual vector is done using one multigrid V-cycle per CG iteration. The MGCG solver developed combines the robustness of conjugate gradient methods with the superior scaling of multigrid methods. The result is that high-resolution simulations can be handled in a reasonable amount of time.

PROBLEM SETUP

The code based on the numerical methods outlined is applied to the flow of liquid over a weir. The problem initialisation is illustrated in Figure 1. At the start of the experiment, all liquid is held back by a gate closing on top of the weir. The gate is lifted at time t = 0, allowing liquid to fall over the weir under gravity. The height of the weir is 200mm, and its width is 12mm. The weir is located 300mm away from the fixed retaining wall. Initially with the gate closed, the heavier fluid is filled to a height of 180mm, ie. 20mm underneath the top of the weir. A lighter liquid layer of depth 50mm is then placed over the top of the heavier layer. The right and bottom walls of the computational flow domain are simulated as no-slip boundaries. Flow dynamics in the air away from

the liquid are relatively unimportant, so the left and top boundaries are simulated as free-slip boundaries. The obstacle itself is treated as a no-slip boundary. The left and top boundaries are located far enough away from the obstacle, such that gas dynamics that develop resulting from the presence of free-slip walls instead of open boundaries have little effect on the liquid flow over the weir. The schematic diagram of the simulation setup is shown in Figure 1 below. The mesh resolution used for the simulations was 256×128 cells.

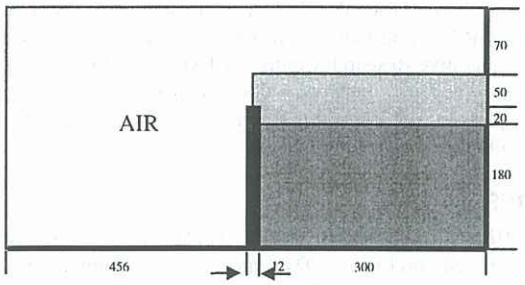

Figure 1 : Schematic diagram of simulation set-up.

Surface tension is not important for this problem, and is neglected. Water is used as an overlying light liquid layer, and a salt solution is used as an underlying heavy liquid layer. Relevant physical property data is given in Table 1 below

	Density (kg/m^3)	Viscosity (cP)
Air	1.204	0.0181
Light liquid	997	0.9997
Heavy liquid	1147	1.75

Table 1: Physical property data.

SIMULATIONS FOR 20mm SUBMERGENCE

Figure 2(a) shows the predicted interfacial profiles at selected times after the gate is opened. Figure 2(b) displays video images of the interfacial profiles at the same times. As can be seen, the numerical and experimental results compare favourably. The top layer is seen to fall over the weir under gravity, initiating a horizontal flow of the top liquid over the weir. The horizontal flow of the top liquid drives the flow of the bottom liquid in the same direction. The bottom liquid adjacent to the weir rises and is entrained in the flow of the top liquid over the weir. This is the only mechanism of entrainment witnessed: no entrainment resulting from Kelvin-Helmholtz instability is apparent. The flow of the heavier bottom liquid over the weir starts to recede after about t = 0.5 sec. Entrainment of the heavier liquid ceases soon after t = 0.8 sec. The liquid-liquid interface adjacent to the weir falls, initiating a back-wave. The liquid-liquid interface on the right side of the weir is faithfully represented, as is the top free surface. This is shown in Figure 3, which compares interfacial positions for given horizontal coordinates obtained from simulation and experiment. As can be seen, the results seen in Figure 3 are in good agreement. The solutions to the velocity fields, pressure distributions and fluid distributions are coupled, as seen in the solution algorithm. Errors in the velocity fields introduce error into the interface tracking. The simulation and experimental interfaces closely correspond after thousands of timesteps in the simulation, suggesting the velocity and pressure solutions are accurate. Future work in measuring the velocity field by PIV techniques is being planned. The results in Figures 2 and 3 validate the numerical schemes used in the code, and enable the code to be used with confidence in analysing the flow of immiscible liquid layers over a weir.

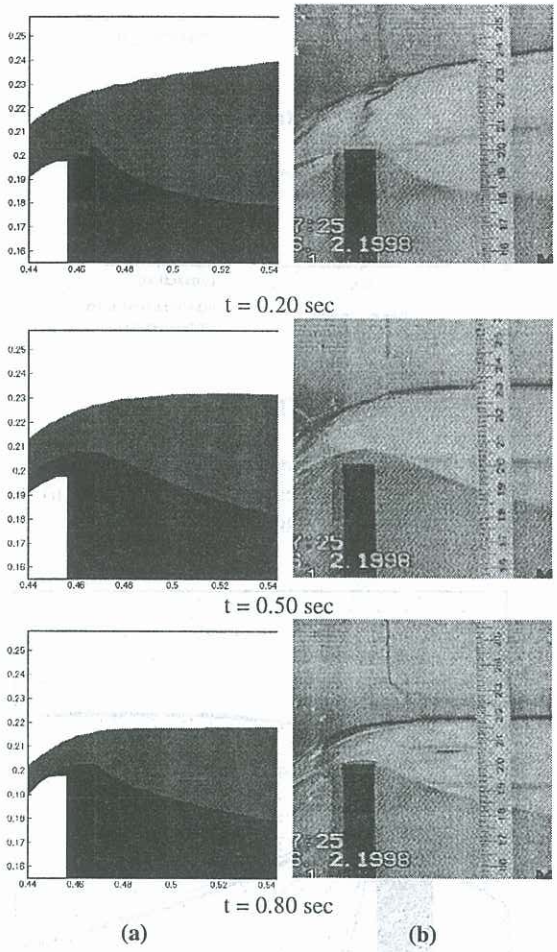

Figure 2: Comparison of (a) numerical and (b) experimental interfacial profiles.

Having validated the numerical method, the code is used to analyse the mechanism of entrainment of the bottom liquid in the flow over the weir. Figure 4 shows the flow field at t = 0.5 sec in more detail, including streamlines, velocity vectors and dynamic pressure contours. Velocity vectors in the liquid are largest in the top liquid as it is about to drop over the weir. This indicates that there is acceleration of the liquid as it falls over the weir. The result is a drop in the pressure of the liquid just above the weir. A pressure gradient is set up between the liquid above the weir and the liquid behind the weir. This is apparent looking at the dynamic pressure contours, with contour levels in the liquid decreasing as the flow approaches the top of the weir. The decreasing pressure gradient accelerates liquid adjacent to the weir in an upward direction, as can be seen by the direction of the streamlines. The pressure gradient is sufficient to take the heavier bottom liquid above the top of the weir. This

bottom liquid is then entrained in the top liquid falling under gravity over the weir.

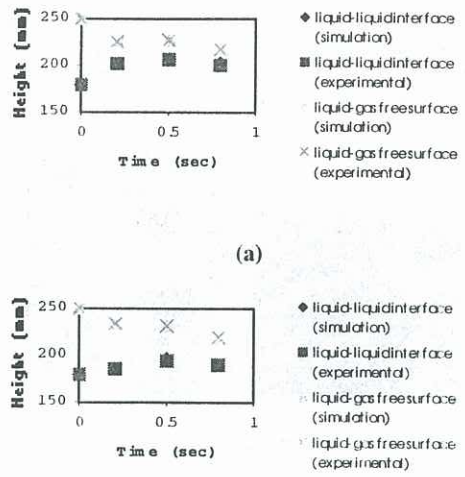

Figure 3: Interfacial positions above the bottom wall for given horizontal coordinates, for **(a)** 0 mm and **(b)** 30 mm from the right wall of the obstacle respectively.

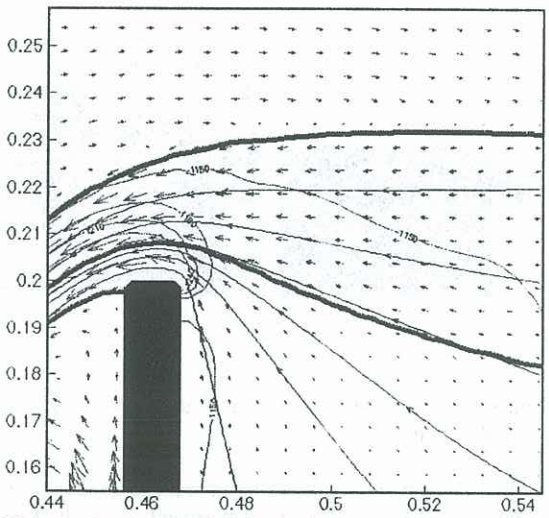

Figure 4: Interfacial profiles, velocity vectors, streamlines and pressure contours for the flow field at t = 0.5 sec.

CONCLUSION

A numerical method has been developed to simulate the flow of immiscible liquid layers over a weir. Experiments of this flow over a weir were run, where a liquid body consisting of a 180 mm thick bottom layer and a 70 mm thick top layer are obstructed from falling under gravity by a 200 mm high and 12 mm wide weir. The code has been validated by comparisons between simulation results and results obtained from video images of the experiments. Entrainment of the bottom liquid in the top liquid is seen despite the liquid-liquid interface initially being below the top of the weir. The code enables us to visualise the mechanism of entrainment of the bottom liquid in the top liquid stream flowing over the weir. The pressure gradient in the liquid adjacent to the weir is sufficiently strong to pull heavier liquid from over 20mm underneath the top of the weir. These results demonstrate the power of the code, and its potential for enabling selective withdrawal of the top liquid to be predicted.

ACKNOWLEDGEMENTS

Financial support for this work was provided by the Australian Minerals Industry Research Association (AMIRA) using facilities provided by the G.K. Williams Cooperative Research Centre for Extractive Metallurgy, a joint venture between CSIRO Minerals and the Department of Chemical Engineering, The University of Melbourne.

REFERENCES

HIRT, C.W. and NICHOLS, B.D., "Volume of Fluid (VOF) Method for the Dynamics of Free Boundaries", *J. Comp. Phys.*, **39**, 201-225, 1981.

KOTHE, D.B., MJOLSNESS, R.C. and TORREY, M.D., *"RIPPLE: A Computer Program for Incompressible Flows with Free Surfaces"*, LA-12007-MS, Los Alamos National Laboratory, 1991.

MORTON, D.E., *"Numerical Simulation of an Impacting Drop"*, PhD Thesis, University of Melbourne, Parkville, 1997.

MORTON, D.E., RUDMAN, M.J. and LIOW, J.-L., "A Finite Difference Method for Modelling Impacting Drops", *The 1997 ASME Fluids Engineering Division Summer Meeting*, June 22-26, ASME, 1997.

RUDMAN, M., "A Volume-Tracking Method for Incompressible Multi-Fluid Flows with Large Density Variations", submitted to the *Int. J. Num. Meth. Fluids*, 1997.

TATEBE, O., "The Multigrid Preconditioned Conjugate Gradient Method", *Proceedings of the Sixth Copper Mountain Conference on Multigrid Methods*, (Eds. N.D. Melson, T.A. Manteuffel and S.F. McCormick), 621-634, 1993.

VAN LEER, B., "Towards the Ultimate Conservative Difference Scheme IV. A New Approach to Numerical Convection", *J. Comp. Phys.*, **23**, 276-299, 1977.

WELCH, J.E., HARLOW, F.H., SHANNON, J.P. and DALY, B.J., *"The MAC Method: A Computing Technique for Solving Viscous, Incompressible, Transient Fluid-Flow Problems Involving Free Surfaces"*, Los Alamos Scientific Laboratory Report LA-3425, 1966.

YOUNGS, D.L., "Time-Dependent Multi-Material Flow with Large Fluid Distortion", *Numerical Methods for Fluid Dynamics*, (Eds. K.W. Morton and M.J. Baines), Academic, 273-285, 1982.